The American Journal of Pathology, Vol. 176, No. 3, March 2010

DOI: 10.2353/ajpath.2010.090735

Epithelial and Mesenchymal Cell Biology

Alternatively Activated Macrophages and Collagen Remodeling Characterize the Postpartum Involuting Mammary Gland across Species

Jenean O'Brien,*† Traci Lyons,* Jenifer Monks,‡§ M. Scott Lucia,¶‖ R. Storey Wilson,¶ Lisa Hines,** Yan-gao Man,†† Virginia Borges,*‖ and Pepper Schedin*†‖‡‡

From the Department of Medicine, Division of Medical Oncology, the Program in Cancer Biology,† the Departments of Physiology and Biophysics,‡ the Webb-Waring Center,§ and the Department of Pathology,¶ University of Colorado Denver, Aurora; the University of Colorado Cancer Center,‖ Aurora; the Department of Biology,** University of Colorado at Colorado Springs, Colorado Springs; the Department of Gynecologic and Breast Pathology,†† Armed Forces Institute of Pathology, and American Registry of Pathology, Washington DC; and the AMC Cancer Research Center,‡‡ University of Colorado Denver, Denver, Colorado*

Recent pregnancy correlates with decreased survival for breast cancer patients compared with non–pregnancy-associated breast cancer. We hypothesize that postpartum mammary involution induces metastasis through wound-healing programs known to promote cancer. It is unknown whether alternatively activated M2 macrophages, immune cells important in wound-healing and experimental tumorigenesis that also predict poor prognosis for breast cancer patients, are recruited to the normal involuting gland. Macrophage markers CD68, CSF-1R, and F4/80 were examined across the pregnancy and involution cycle in rodent and human mammary tissues. Quantitative immunohistochemistry revealed up to an eightfold increase in macrophage number during involution, which returned to nulliparous levels with full regression. The involution macrophages exhibit an M2 phenotype as determined by high arginase-1 and low inducible nitric oxide synthase staining in rodent tissue, and by mannose receptor expression in human breast tissue. M2 cytokines IL-4 and IL-13 also peaked during involution. Extracellular matrix (ECM) isolated from involuting rat mammary glands was chemotactic for macrophages compared with nulliparous mammary ECM. Fibrillar collagen levels and proteolysis increased dramatically during involution, and denatured collagen I acted as a strong chemoattractant for macrophages in cell culture, suggesting proteolyzed fibrillar collagen as a candidate ECM mediator of macrophage recruitment. M2 macrophages, IL-4, IL-13, fibrillar collagen accumulation, and proteolysis of collagen are all components of tumor promotional microenvironments, and thus may mediate promotion of breast cancers arising in the postpartum setting. ***(Am J Pathol 2010, 176:1241–1255; DOI: 10.2353/ajpath.2010.090735)***

Although it is recognized that full-term pregnancy at an early age reduces the lifetime risk of developing breast cancer, women of all ages have a transient increase in breast cancer risk with a recent pregnancy.[1–4] Breast cancers diagnosed up to five years out from a completed pregnancy have been referred to as pregnancy-associated or PABC.[5,6] Several studies have shown that PABC frequently metastasizes, resulting in poor prognosis for the patient.[6–8] Epidemiological data identify women whose breast cancer is diagnosed postpartum, rather than during pregnancy, as having the worst outcomes.[7–14] Further, when breast cancer patients were matched for known prognostic indicators, the postpartum window proved to be an independent factor for metastasis, whereas a diagnosis during pregnancy did not.[11,14,15] We have proposed the involution-hypothesis to account for the high metastatic oc-

Supported by grants from Department of Defense Synergistic Idea Award #BC060531, University of Colorado Cancer Center Seed grant, Avon Foundation grant and Women's Health and Gender Based Disease grant (to P.S. and G.B.), a Department of Defense Predoctoral grant #BC073482 (to J.O.), and an American Cancer Society New England Division Postdoctoral Fellowship Spin Odyssey #PF-08-257-01-CSM (to T.L.).

J.O. and T.L. contributed equally to this work.

Accepted for publication October 29, 2009.

Supplemental material for this article can be found on *http://ajp.amjpathol.org*.

Address reprint requests to Pepper Schedin, Ph.D., Division of Medical Oncology, Mail Stop 8117, RC-1 S, 8401K, 12801 E. 17th Avenue, UCD, Aurora, CO 80045. E-mail: Pepper.Schedin@UCDenver.edu.

currence of PABC diagnosed during the postpartum window.[5,16–18] Specifically, we predict that the involuting microenvironment, with its similarities to wound and cancer environments, supports dissemination of pre-existing but previously quiescent tumor cells. In support of this hypothesis, we have shown that extracellular matrix (ECM) proteins isolated from the involution microenvironment have wound healing characteristics and are promotional for breast tumor cell metastasis.[16] We extend our studies to address whether alternatively activated M2 macrophages, an immune cell type implicated in wound healing and breast cancer metastasis, participate in postpartum gland regression.

Postpartum mammary gland involution is a necessary physiological process required to return the lactation competent gland to a nonlactating state poised to respond to a subsequent round of pregnancy. In rodent models, weaning-induced milk stasis triggers cessation of milk secretion and the milk-producing secretory alveoli that developed during pregnancy are rapidly resorbed. In rodent models, it has been shown that 50% to 80% of the secretory mammary epithelium is eliminated by apoptosis within the first week of involution.[19,20] This dramatic tissue remodeling requires two major processes: apoptotic death of the mammary epithelial cells and stromal activation.[21] Accumulating evidence in rodents indicates that tissue-remodeling programs similar to wound healing are used to remodel the lactating gland to its postpartum state. Similarities include elevated levels of the immunomodulators transforming growth factor (TGF)-β1 and 3, increases in matrix metalloproteinase (MMP)-2, −3, and −9, deposition of fibrillar collagens, presence of bioactive proteolytic fragments of the ECM proteins fibronectin and laminin, as well as gene expression profiles consistent with activation of innate and adaptive immunity.[22–25]

Macrophages are a dynamic population of immune cells recognized for their contribution to wound resolution through phagocytosis and for their role in antigen presentation. The detailed functions of macrophages are extensive, as their precursor cells can respond to a variety of physiological situations and mature along a spectrum of phenotypes. The M1/M2 macrophage nomenclature system described by Mantovani and colleagues[26] primarily divides cells based on production of Th1 versus Th2 cytokines. According to this classification, the M1-type, or classically activated macrophages, mature in response to signaling molecules elicited by intracellular pathogens including lipopolysaccharide, interferon-γ and -β, and TNF-α. These M1 macrophages respond in kind by producing Th1 cytokines including interleukin (IL)-12 and IL-23 that subsequently promote activation of cytotoxic T-lymphocytes. M1 macrophages are involved in antigen presentation, immune surveillance, and killing of cells with foreign antigens, including tumor cells.[26–28]

On the other end of the spectrum, M2 macrophages are alternatively activated by Th2 cytokines such as IL-4, IL-13, and the immunosuppressive IL-10.[26] M2-type macrophages in turn produce Th2 cytokines. M2 macrophages participate in wound healing and tissue repair through activities including phagocytic debris clearance, release of TGF-β and fibronectin, and release of PDGF and VEGF,[27,29] which promote angiogenesis. Recently, it has become apparent that macrophages are functionally plastic, in that they respond to their environment with heterogeneous and transient phenotypes that are not distinctly divided into the M1/M2 categories.[30]

Several recent reviews highlight shared characteristics of M2 macrophages and tumor-associated macrophages (TAMs).[26,31] TAMs are important in the progression of mammary cancer in several rodent models.[32,33] The observed similarities between TAMs and M2 macrophages suggest that M2 macrophages may also have tumor promotional capabilities.[34] Further, clinical data reveals that macrophage chemotactic factors, macrophage growth factors, and macrophage infiltration all correlate with negative outcomes for breast cancer patients.[35–40] TAMs and M2 macrophages are thus implicated as key mediators of breast cancer progression.

Based on evidence that macrophages promote breast cancer and that the wound-healing microenvironment of the involuting rodent mammary gland is tumor promotional, we evaluated whether macrophages characterize the postpartum involuting mammary gland. Here we demonstrate an influx of macrophages during postlactational involution, identified as consisting primarily of M2 macrophages in rodents and humans. Further, we provide a plausible mechanism for macrophage recruitment via their attraction to the ECM protein collagen I. These observations are consistent with our previous data demonstrating that the involuting rat mammary gland is characterized by a wound healing microenvironment and extends these findings to human breast tissues. These data further support the hypothesis that postpartum involution promotes tumor progression and accounts for the poor prognosis of PABC.

Materials and Methods

Rodent Breeding and Tissue Preparations

Sprague–Dawley rats and C57BL/6 mice from Taconic Farms (Germantown, NY) were bred at seven to ten weeks of age. All rodents were housed in microisolator cages and subjected to 12-hour light/dark cycles, with water and LabDiet-5020 provided *ad libitum*. Within two days postparturition litter sizes were standardized to eight pups. Pups were removed at lactation day 10 (rats) or day 14 (mice). Rats were euthanized by CO_2 asphyxiation, whereas mice were anesthetized with sodium pentobarbital (0.1 mg/g body weight) and intracardially perfused with 20 ml ice-cold PBS (with Ca^{2+}/Mg^{2+}) followed by 20 ml each of 2% and 4% PFA in PBS (with Ca^{2+}/Mg^{2+}). In rats, mammary gland tissue was collected from mid-pregnant, days 0 (day of pup withdrawal for lactation group), 2, 4, 6, 8, 10 (involution group), and 60 postweaning (regressed group). In mice, mammary gland tissue was harvested on days 0 (day of pup withdrawal for lactation group), 1, 2, 3, 4, 5 (involution group), and 21 (regressed group) postweaning. Mammary gland tissue was also obtained from age-matched nulliparous animals. In the rats, daily cervical lavages were performed

starting one week before euthanasia for the nulliparous and regressed groups, and these animals were sacrificed during estrus to control for potential variations in ECM composition attributable to differences in stage of estrous. LN-free rat mammary glands #4 to 6 were taken for subsequent matrix isolation and biochemical analyses, flash frozen, and stored at −80°C. Rat mammary gland tissue associated with the LN region was fixed in 10% neutral buffered formalin for 24 hours and paraffin embedded for histological analysis. Reproductive state was verified by histological analysis of cervical specimens as previously described.[41] H&E stain of mammary and cervical tissues was performed according to published methods.[42] For the mouse studies, one #4 mammary was removed, weighed, fixed in 4% PFA for 4 hours, and embedded in paraffin for histological analysis. The IACUC of University of Colorado Denver approved all procedures.

Human Tissue Acquisition

All research using human materials was conducted under a protocol approved by the Colorado Multiple Institution Review Board (COMIRB) and United States Army Medical Research and Materiel Command's (USAMRMC) Office of Research Protections (ORP) Human Research Protection Office (HRPO). All cases were deidentified to the research team. Also, the protocol was deemed exempt from subject consent and Health Insurance Portability and Accountability Act (HIPAA) authorization. Three types of tissue were collected. The first, human breast cancer cases diagnosed during pregnancy, lactation, or involution, were retrospectively identified from the tumor registry of Colorado based on women age 45 or younger, with a diagnosis of invasive breast cancer. The second, cases without cancer, were identified based on reproductive stage at the time of tissue collection, which subsequently revealed no malignancy, or on pathology reports that revealed no malignancy and which indicated lactational changes. The third set were nulliparous or fully involuted from the lactational state, here defined as regressed, tissues obtained from a subset of women who were Colorado participants in the 4-Corners Breast Cancer Study, a population-based case–control study of breast cancer. Briefly, women who were 25-79 years old at breast cancer diagnosis were recruited from the Southwest United States (AZ, CO, NM, UT) between the years of 2000 to 2005. Cases with a breast cancer diagnosed in October 1999 to May 2004 were identified through statewide cancer registries. Methods for selection, recruitment, and interview of subjects have been previously described in detail.[43] All aspects of the 4-Corners Study were conducted in accordance with human subjects' research protocols approved at each institution. Cases included in this present study were women who were diagnosed with invasive breast cancer at the age of 45 or younger ($n = 68$). Pathology reports, subject interview questionnaires, and the tumor registry were used to obtain reproductive history and clinical data on standard breast cancer prognostic markers. For all three tissue sets, nulliparous cases were from women who had never been pregnant and had cancer. Pregnant and lactation cases were from women who were either pregnant or still lactating at the time of tissue collection, as indicated from chart review. Involution cases were from women who had recently been, but were no longer, lactating. Regressed cases were from women who were at least 10 years out from their last pregnancy and had breast cancer. Number (n) of cases, average age ($\bar{a}$) and fields (f) total number for each developmental stage: CD45 (for details see Supplemental Table S1 at *http://ajp.amjpathol.org*), nulliparous $n = 5$, $\bar{a} = 34$, f = 58; pregnant $n = 8$, $\bar{a} = 30$, f = 81; lactation $n = 11$, $\bar{a} = 30$, f = 129; involution $n = 8$, $\bar{a} = 30$, f = 116; and parous/regressed $n = 10$, $\bar{a} = 42$, f = 81. CD68 (for details see Supplemental Table S2 at *http://ajp.amjpathol.org*), nulliparous $n = 6$, $\bar{a} = 35$, f = 67; pregnant $n = 9$, $\bar{a} = 27$, f = 86; lactation $n = 9$, $\bar{a} = 31$, f = 129; involution $n = 8$, $\bar{a} = 31$, f = 130; and parous/regressed $n = 8$, $\bar{a} = 43$, f = 95.

Immunohistochemistry, Imaging, and Quantification

Four-μm sections of paraffin embedded rodent mammary gland or human breast tissues were pretreated in Dako TRS Antigen Retrieval Solution (AR1) or Dako EDTA Antigen Retrieval Solutin (AR2) at 125°C under pressure for five minutes, or with Proteinase K (Dako) for three minutes at room temperature (AR3). For frozen tissue, sections were removed from the freezer and allowed to air dry two to five minutes before fixation in cold 70% ethanol for five minutes. For rodent tissues the following antibodies, antigen retrievals, and antibody dilutions were used: CD68 (AR1 1:100, AbD Serotec, Raleigh, NC), CSF-1R (AR2, 1:100, Abcam, Cambridge, MA), F4/80 (AR1, 1:100, AbD Serotec), iNOS (AR1, 1:50 in rat, 1:100 in mouse, BD Biosciences, San Jose, CA), Arginase-1 (AR1, 1:100 in rat, 1:500 in mouse, Santa Cruz, Santa Cruz, CA). For human tissues the following antibodies, antigen retrievals, and antibody dilutions were used: CD68 (AR1, 1:1000, Dako), CK18 (AR2, 1:100, Epitomics, Burlingame, CA), CD45 (AR1, 1:200, Dako), IL-13 (AR3, 1:50, Abcam, Cambridge, MA), and mannose receptor on frozen tissue sections (Abcam). Immunoreactivity was detected using Envision+ Systems (Dako) for mouse, rat, and rabbit primary antibodies or Vectastain Elite ABC Kit (Vector Labs, Burlingame, CA) for goat primary antibodies. 3,3′-diaminobenzidine was used as the chromagen in all tissues. For animal tissues, positive stromal cells were quantified in 6 fields per animal at ×400, $n = 4$ rats or $n = 2$ to 4 mice per time point.

For human tissues positive cells were quantified in collaboration with the UCD Prostate Cancer Research Laboratory, which has developed a novel approach for the analytical study of histological sections using computer assisted image analysis.[44,45] Briefly, entire histological sections were imaged with Aperio ScanCope T3 scanner at 0.47 microns/pixel. The images were then down-sampled to a resolution of 1.5 microns per pixel to facilitate subsequent image manipulation. Using Adobe

Photoshop CS2 software, 10 lobuloalveolar fields/case/reproductive stage were isolated. Color threshold image analyses specific for CD45 and CD68 immunostains were then performed using custom written plugins for Image J software[46] and percent positive pixels for CD45 or CD68 immunostain determined.

Immunofluorescence

Four-μm sections of paraffin-embedded human breast tissue was pretreated (see above) and coincubated with primary antibodies for E-cadherin (AR1, 1:300, Santa Cruz) and CD68 (AR1, 1:1000, Dako). The following fluorescent secondary antibodies were used: Alexa Fluor® 488 goat–anti-rabbit IgG (H+L) and Alexa Fluor® 594 goat–anti-mouse IgG (H+L) (Invitrogen, Carlsbad, CA). Slides were mounted using VECTASHIELD® Mounting Medium with DAPI (Vector Labs). Images were captured using a Zeiss Axioskop microscope equipped with an HBO 100 lamp and photographed by a digital camera (SPOT RTke, SPOT Diagnostics).

Mammary ECM Isolation

Matrix isolation was performed as previously described[41] and based on published protocols.[47,48] Briefly, frozen #4 to 6 LN-free rat mammary glands were pulverized and homogenized in a high salt/N-ethylmaleimide (NEM) solution (3.4 M NaCl, 50 mmol/L Tris-HCl pH 7.4, 4 mmol/L EDTA, 2 mmol/L NEM) containing proteinase inhibitor cocktail (200 μg/ml, Sigma) at 4°C. Lysates were enriched for ECM by 2 cycles of centrifugation (RCF_{max} 110,000 $\times$ *g*, 30 minutes, 4°C), with pellets resuspended in high salt/NEM buffer. ECM enriched pellets were resuspended in mid-salt/urea solution (2 mol/L urea, 0.2 M NaCl, 50 mmol/L Tris-HCl pH 7.4, 4 mmol/L EDTA, 2 mmol/L NEM) with proteinase inhibitor cocktail and agitated overnight at 4°C. Samples were centrifuged at RCF_{max} 110,000*g*, and the ECM-enriched supernatants dialyzed for 48 hours (molecular weight cutoff 12 to 14 kDa, Spectrum) against low salt buffer (0.15 mol/L NaCl, 50 mmol/L Tris-HCl pH 7.4, 4 mmol/L EDTA), and against sera-free media for 24 hours (DMEM/F12 media (Sigma) supplemented with 1 μg/ml Gentamicin) at 4°C. Matrices were used within two weeks of isolation and stored on ice at 4°C. ECM protein integrity was shown to be stable under these storage conditions (data not shown). For each ECM preparation, mammary glands were pooled from five to six rats per group. Two separate preparations of mammary matrix were evaluated in chemoattractant assays.

Cell Chemoattractant Assays

The J774 mouse macrophage cell line derived from a tumor in a BALB/c mouse, and graciously obtained from Doug Graham, (Pediatric Hematology and Oncology, University of Colorado Denver) was cultured in DMEM with 10% FBS at 10% CO_2. All chemoattractants including gelatin (Sigma, St. Louis, MO), fibrillar rat tail collagen 1 (BD Biosciences, Sparks, MD) and isolated mammary ECM were diluted with sera-free media to 7 μg/ml and plated in a final volume of 800 μl/well in the bottom of 24-well transwell assay plates. Ten percent FBS was used as a positive control, and each condition was performed in triplicate. J774 cells were rinsed once with PBS, resuspended in sera-free DMEM, and plated 100,000 cells/well in a 200 μl volume on top of the filters in 24-well transwell assay plates. These plates were placed in the incubator for 8 hours, then fixed in 10% neutral buffered formalin and stained with 0.1% crystal violet. Nonmotile cells were scraped off the top of the filter, and images of each filter taken at $\times$400. Cells that had migrated to the bottom of the filter were counted using four representative quadrants of each image. Each assay was repeated three to four times, with data trends consistent between repeats.

Collagen Detection and Quantification

For detection of fibrillar collagen in human tissues, 5-μm sections of lactating and actively involuting breast tissue were stained using Ventana Trichrome III Blue Staining Kit, which is a modification of Masson trichrome method, on the Ventana NexES® Special Stain automated stainer. For detection of fibrillar collagen in rat tissues, 5 μm sections of rat mammary tissues were stained with Sirius Direct Red 80 (Sigma) and counterstained with Hematoxylin according to published methods.[42] Collagen quantitation of human and rat samples were performed in the UCHSC Prostate Diagnostic Laboratory as described above. Using this software 25 lobuloalveolar structures from each human tissue were isolated from each $\times$400 slide image (n = 4 for lactation and involution) and percent composition determined by number of blue pixels in each structure. For intralobular collagen quantification of rat tissue, 10 alveolobular structures were isolated from each slide (n = 3), the lumen were excluded, and percent composition of light red pixels determined. Interlobular collagen was quantified by isolating the dark red signal from the scanned section in total.

Zymogen Assay

Substrate gel analyses were performed as previously described.[17] Briefly, equal amounts of protein (20 μg) from each tissue sample were run under nonreducing conditions on a 7.5% SDS-PAGE gel containing 3 mg/ml of porcine gelatin (Sigma), followed by incubation of the gel in a shaking water bath at 37°C for 72 hours in substrate buffer (50 mmol/L Tris-HCl, pH 8.0, 5 mmol/L $CaCl_2$). Proteinase activity was visualized by Coomassie Blue R250 staining and zymogen activity appeared as a cleared band on a dark background.

Collagen Western Blot Analysis

Collagen 1 was detected by Western blot as previously described.[49] Briefly, 3% polyacrylamide (29:1) gels were prepared using 9.2 mmol/L calcium lactate, pH 6.8; 0.1% TEMED; and 0.07% ammonium persulfate only and pre-

run for 1.5 hours at 100 volts with 50 mmol/L Tris, pH 6.6 lactic acid buffer in the cathode region and 0.1 mol/L lactic acid, pH 2.5 in the anode region with reversed electrodes. Mammary ECM samples from involution day 4 to 6 rats were prepared in 0.1 mol/L lactic acid, pH 2.5, and run for 2.5 hours at 70 volts with reversed electrodes. Collagens were transferred with nylon mesh between the gel and nitrocellulose in 0.1 mol/L lactic acid, pH 2.5 at 20 volts overnight at room temperature, with reversed electrodes. Collagen-1 was detected by primary antibody (1:500, Abcam) and anti-rabbit Hrp conjugate secondary antibody (1:5000 Jackson Immunochemical, West Grove, PA). Signal was obtained using ECL western detection kit (Amersham).

Cytokine Array

Rat mammary tissue was lysed in 20 mmol/L Tris-HCl, pH 7.5, 150 mmol/L NaCl, 0.05% Tween-20, 200 μg/ml PMSF, and proteinase inhibitor cocktail. Lysates were analyzed using a Milliplex Rat Cytokine Immunoassay Kit (Millipore, Billireca, MA) for monocyte chemotactic protein-1 (MCP-1), IL-4 and IL-13 and collected on a Luminex Multiplex Instrument in the University of Colorado Cancer Center Flow Cytometry Core Facility.

Results

Macrophage Influx into Involuting Rodent Mammary Gland

A wound healing gene signature consistent with macrophage recruitment and evidence for macrophage influx have been identified in the involuting mouse mammary gland.[23,24,50] We therefore analyzed whether macrophage influx was specific to mice or could be generalized to mammary involution across different species by quantifying two macrophage markers by immunohistochemistry (IHC). CD68 is a macrophage lysosome-associated protein[51] and CSF-1R is the receptor for CSF-1, a cytokine that promotes monocyte maturation and differentiation.[52] The number of CD68-positive cells was evaluated in the rat at day 6 postweaning (involution day 6), which corresponds to the peak of tissue remodeling during mammary involution.[21,49] Stromal associated CD68 levels were sixfold higher at involution day 6 compared with mammary glands from age-matched nulliparous rats (Figure 1A). Similarly, the number of CSF-1R–positive cells was increased eightfold on involution day 6 when compared with nulliparous controls (Figure 1B). Of interest, the number of CSF-1R–positive cells was considerably lower than the number of CD68-positive cells, suggesting many stromal CD68-positive cells are CSF-1R negative. These data are consistent with previously reported results indicating that distinct macrophage populations stain differentially for these two markers.[53–56] To determine whether the increase in macrophage density in the involuting tissue was attributable to influx rather than their concentration after alveoli collapse, Western blot analysis was performed on mammary lysates loaded at equal protein concentration (Figure 1C). We observed an increase in CD68 protein levels during mammary involution, suggesting that the increase in CD68+ cells

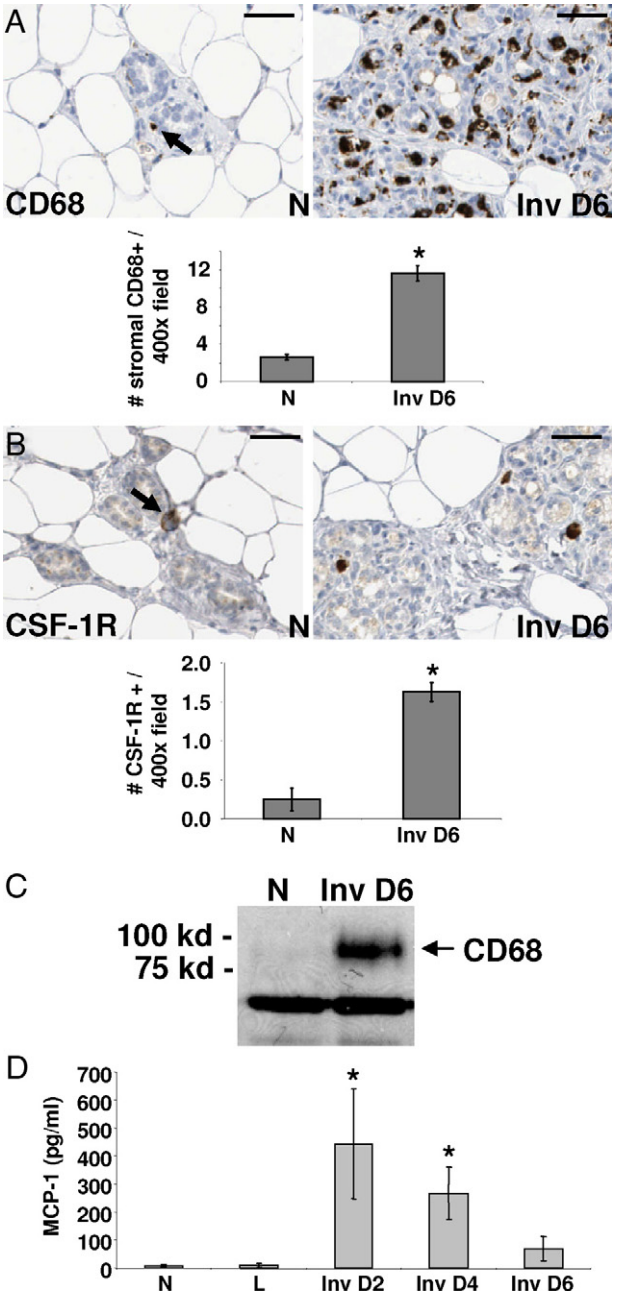

Figure 1. Macrophage markers increase during mammary gland involution in the rat. **A:** IHC stain for CD68+ cells (**arrow**) in mammary glands from nulliparous (N) or involution day 6 (Inv D6) rats and quantified per ×400 field/10 fields per gland, $n = 4$ rats per stage, $^*P < 0.0001$, unpaired t test; scale bars represent 50 microns. **B:** IHC stain for CSF-1R+ cells (**arrow**) in mammary glands from nulliparous (N) or involution day 6 (Inv D6) rats and quantified per ×400 field/10 fields per gland, $n = 4$ rats per stage, $^*P = 0.0022$, unpaired t test; scale bars represent 50 microns. **C:** Western blot for CD68 using mammary tissue lysates from nulliparous (N) or involution day 6 (Inv D6) rats, $n = 6$ rats per stage. IgG is used as a loading control. **D:** Immunoassay results for monocyte chemotactic protein (MCP-1) using rat mammary tissue lysates from nulliparous (N), lactation (L), and involution days 2, 4, and 6 stages, $n = 6$ rats per stage, $^*P < 0.03$ compared with N, Unpaired t-test.

was attribtuable to cell influx rather than tissue collapse. Supportive of macrophage influx, we detected an increase in MCP-1 during involution at 2, 4, and 6 days postweaning compared with nulliparous and lactating rat mammary tissue (Figure 1D). Cumulatively, these results demonstrate an influx of at least two populations of macrophages into the involuting rat mammary gland, CD68-positive/CSF-1R–negative and CSF-1R–positive, which may be mediated in part by MCP-1 expression.

Involution Macrophages Are of the M2 Phenotype

For our initial studies to determine phenotypes of the macrophages present in the mammary gland during involution, we pursued markers of traditionally defined functional populations of M1 and M2 subtypes. Classical M1 macrophages are thought to be tumor suppressive, whereas alternatively activated M2 macrophages are potentially tumor promotional.[26,27] iNOS expression was used to identify rodent M1 subtype, whereas arginase-1 was used to identify the M2 subtype.[27] In rat mammary glands, the expression level of the M1 macrophage marker iNOS was constant across the pregnancy-lactation-involution cycle, whereas the M2-associated arginase-1 expression increased six-fold during involution (Figure 2, A and B). Peak levels of arginase-1 expression were observed during the peak of tissue remodeling in the rat, which occurs at involution day 6.[41] The arginase-1–expressing cells appear to account for the majority of the stromal CD68 staining, demonstrating that most macrophages in the involuting rat mammary gland express the M2 marker, arginase-1 (Figure 2B). Further, cytokine analysis revealed that the levels of IL-4 and IL-13, both M2-associated cytokines,[26] increase during involution with peak levels observed at involution day 4 (Figure 2, C and D). Altogether these data suggest that the involution mammary microenvironment of the rat displays wound-healing traits including the presence of M2 macrophages and cytokines.

Although it has already been demonstrated that macrophages increase in number during mouse mammary gland involution, the question of whether these macrophages are of the M1 or M2 type has not been reported.[40,50] We examined the presence of macrophages in involuting mouse tissue, as identified by F4/80 expression, and discovered a peak increase during involution at

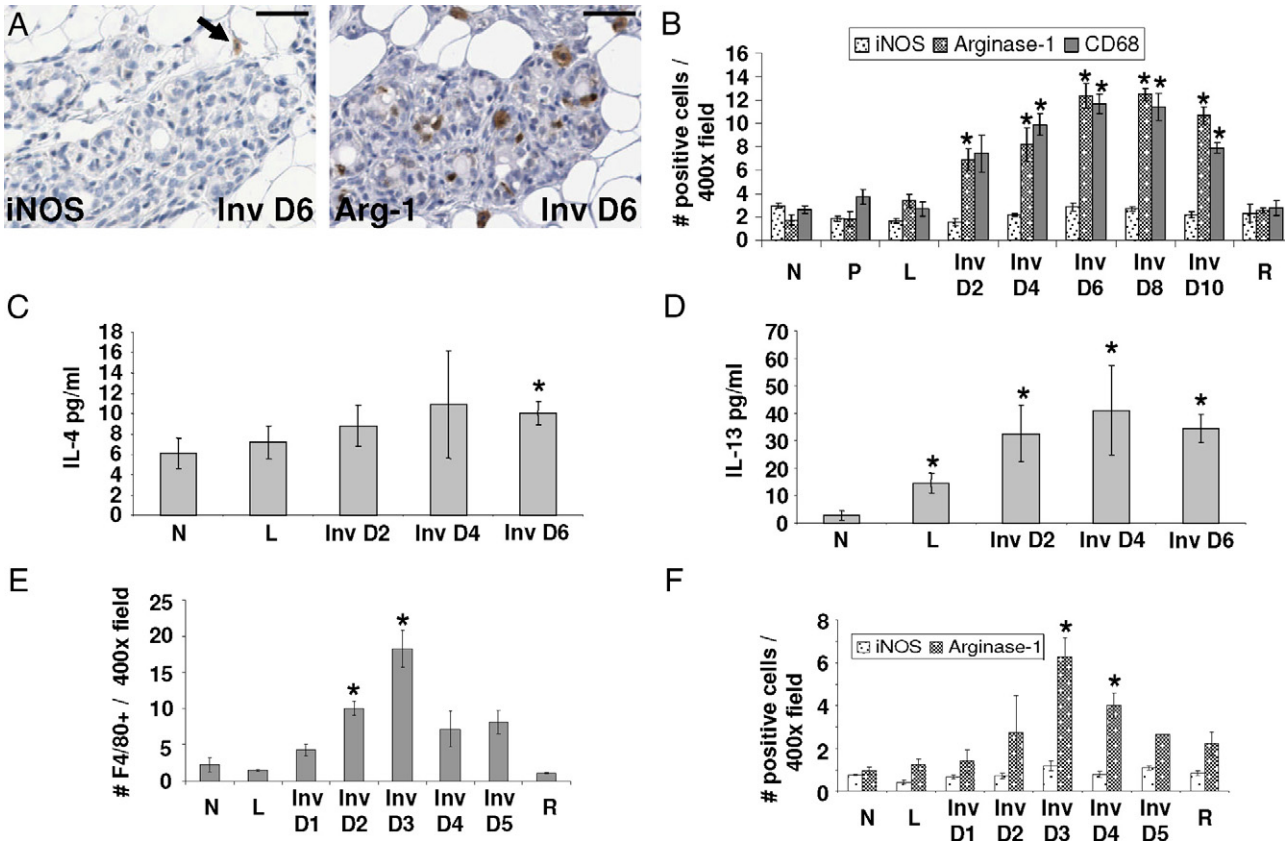

Figure 2. Involution macrophages display an M2-tumor promotional phenotype. **A:** IHC stain for M1 macrophage marker iNOS (**arrow**) and M2 macrophage marker Arginase-1 in involution day 6 (Inv D6) rat mammary tissue; scale bars represent 50 microns. **B:** Quantification of iNOS, Arginase-1, and CD68 IHC stain in rat mammary tissue per ×400 field/10 fields per gland, $n = 4$ rats per stage, $^*P < 0.005$ compared with N, unpaired t test. (N indicates nulliparous; P, pregnant; L, lactation; Inv D, involution day; R, regressed). **C:** Immunoassay results for M2 cytokine IL-4 using rat mammary tissue lysates, $n = 6$ rats per stage, $^*P < 0.05$ compared with N, unpaired t-test. **D:** Immunoassay results for M2 cytokine IL-13 using rat mammary tissue lysates, $n = 6$ rats per stage, $^*P < 0.05$ compared with N, unpaired t test. **E:** Quantification of mouse macrophage marker F4/80 IHC stain per ×400 field/10 fields per gland, $n = 2$ for L, Inv D5; $n = 3$ for Inv D1, D4; $n = 4$ for N, Inv D2, D3 R; $^*P < 0.005$ compared with N, unpaired t test. **F:** Quantification of iNOS, Arginase-1 IHC stain in mouse mammary tissue per ×400 field/10 fields per gland, $n = 2$ for L, Inv D5; $n = 3$ for Inv D1, D4; $n = 4$ for N, Inv D2, D3, R; $^*P < 0.005$ compared with N, unpaired t test.

three days postweaning (Figure 2E). This peak corresponds with the active tissue remodeling phase of involution in the C57/BL6 mouse, where the rate of involution is reported to be faster than in the rat.[50] Next, we determined that the number of macrophages expressing the M2 marker arginase-1 increased sixfold with involution while the number of macrophages expressing the M1 marker iNOS remained low at all stages (Figure 2F). These data demonstrate that the macrophages observed in mouse mammary glands, like those observed in the rat, peak during the active tissue remodeling phase of involution and exhibit an M2-like phenotype. Of note, in the mouse mammary gland, the number of M1 (iNOS-positive) plus M2 (arginase-1–positive) macrophages was lower than the total number of F4/80 macrophages, suggesting the presence of an additional murine F4/80 positive macrophage population that is not activated to express iNOS or Arg-1 (Figure 2, E and F). In contrast, in the rat, the CD68+ macrophages appear to nearly all be activated to iNOS or Arg-1–positive status (Figure 2B). Given that the markers used to identify the macrophage population differed between species, it is not yet possible to directly compare the relative number of unmarked macrophage populations between rat and mouse.

Human Breast Involution

Although mammary involution has been examined extensively in rodent models, the biology of human breast involution has not been systematically studied, primarily because of limited tissue availability. To this end, breast specimens were obtained from women, 45 years of age or younger, who were nulliparous, pregnant, lactating, weaning/involuting, or whose breasts were fully regressed/parous (defined here as fully involuted from the lactational state and >10 years post pregnancy). Representative H&E images of these reproductive stages are shown in Figure 3A. The histological changes that occur with pregnancy, lactation, and involution in human breast tissue appear very similar to published images depicting these same reproductive stages in the rodent.[49,57–60] However, in women, nulliparous and postpartum regressed/parous breast tissue had elevated levels of dense stroma and reduced adipocyte content when compared with equivalent stages of rat and mouse mammary tissue. These findings are consistent with previous reports.[58–60] To examine immune cell composition and macrophage influx, tissue sections from these human breast specimens were analyzed for CD45 and CD68 expression, respectively. CD45, or leukocyte common antigen, is present on the surface of nucleated hematopoietic cells including B-cells, T-cells, neutrophils, and macrophages, and is commonly used as a marker for inflammation.[61] Representative images depicted in Figure 3B show a low number of CD45-positive cells in the nulliparous, pregnant, lactating, and fully regressed/parous human breast tissue. In contrast, CD45 expression is significantly increased in the involuting breast. Similar staining patterns were observed for CD68, the lysosomal marker of macrophages described above (Figure 3C). To semiquantitate CD45 and CD68 marker expression across the pregnancy-lactation-involution panel, we used a computer-assisted image analysis program that captures images of entire histological sections at high resolution, converts the IHC signal to grayscale, and calculates the percent positive signal for each marker. Using this technology, CD45 expression was found to increase fourfold in actively involuting lobules (Figure 3D). An increase in CD68 expression over nulliparous was also observed, however the rise in CD68 levels occurred earlier during pregnancy and lactation. Consistent with the CD45 expression pattern, the highest CD68 levels were observed during involution (Figure 3E). For both markers, signal intensity decreased to prepregnant levels after postpartum involution demonstrating the peak immune-cell signal corresponded with active involution.

To confirm that the CD45 and CD68 IHC signals were specific to immune cells, and not phagocytic mammary epithelial cells, serial sections were stained for CD45, CD68, and CK18, an epithelial cell–specific cytokeratin. Stromal associated CD45 and CD68 double-positive cells (arrowhead) were consistently identified as negative for CK18, strongly suggesting that these cells are indeed immune in origin (Figure 3F, middle panel). In addition, CD45-positive cells that were CD68-negative (left panel, arrow), as well as CD68-positive cells that were CD45-negative (right panel, arrow), were present. These observations indicate additional complexity of the mammary immune cell milieu during involution (Figure 3F). As an independent assessment to confirm that the CD68 IHC signal was identifying macrophages, epithelial cells were identified by E-cadherin expression and macrophages by CD68 using dual immunofluorescence-based IHC. This analysis confirmed the presence of CD68-positive and E-cadherin–negative cells in very close proximity to the involuting E-cadherin–positive epithelium, clearly identifying macrophage presence in the involuting human breast (Figure 3G, arrows). Finally, based on the number of cells in involuting tissue that express macrophage mannose receptor and IL-13, a marker for M2 macrophages in humans and an M2-associated cytokine, we conclude that macrophages with an M2 phenotype are abundant in the human involuting mammary gland (Figure 3H, arrows).[26,27,62]

The breast tissues used for these studies were obtained from women who were subsequently diagnosed with cancer or found to be without evidence of malignancy. It might be anticipated that normal adjacent human breast tissue taken from the women with breast cancer would have higher levels of M2 macrophages present throughout the gland and, further, that these cases account for the higher levels of immune cells observed in the involuting human breast tissues depicted in Figure 3, D and E. First, in an attempt to minimize this confounder, lobules were taken from areas of the breast specimens that were morphologically normal but distinct from the tumor. Such 'normal adjacent' lobules obtained from women with cancer did not

have elevated CD45 staining compared with lobules obtained from women without cancer (Figure 3I). Thus, it does not appear that cancer contributed to the influx of immune cells into the normal adjacent human involuting breast tissues, but rather the influx correlates with the process of involution. Cumulatively, these observations demonstrate that immune cells and M2 macrophages in particular are resident at high levels in the microenvironment of human involuting breast tissue. When combined with the rodent data, these results indicate that infiltration of immune cells is a common characteristic of postpartum mammary gland involution across species.

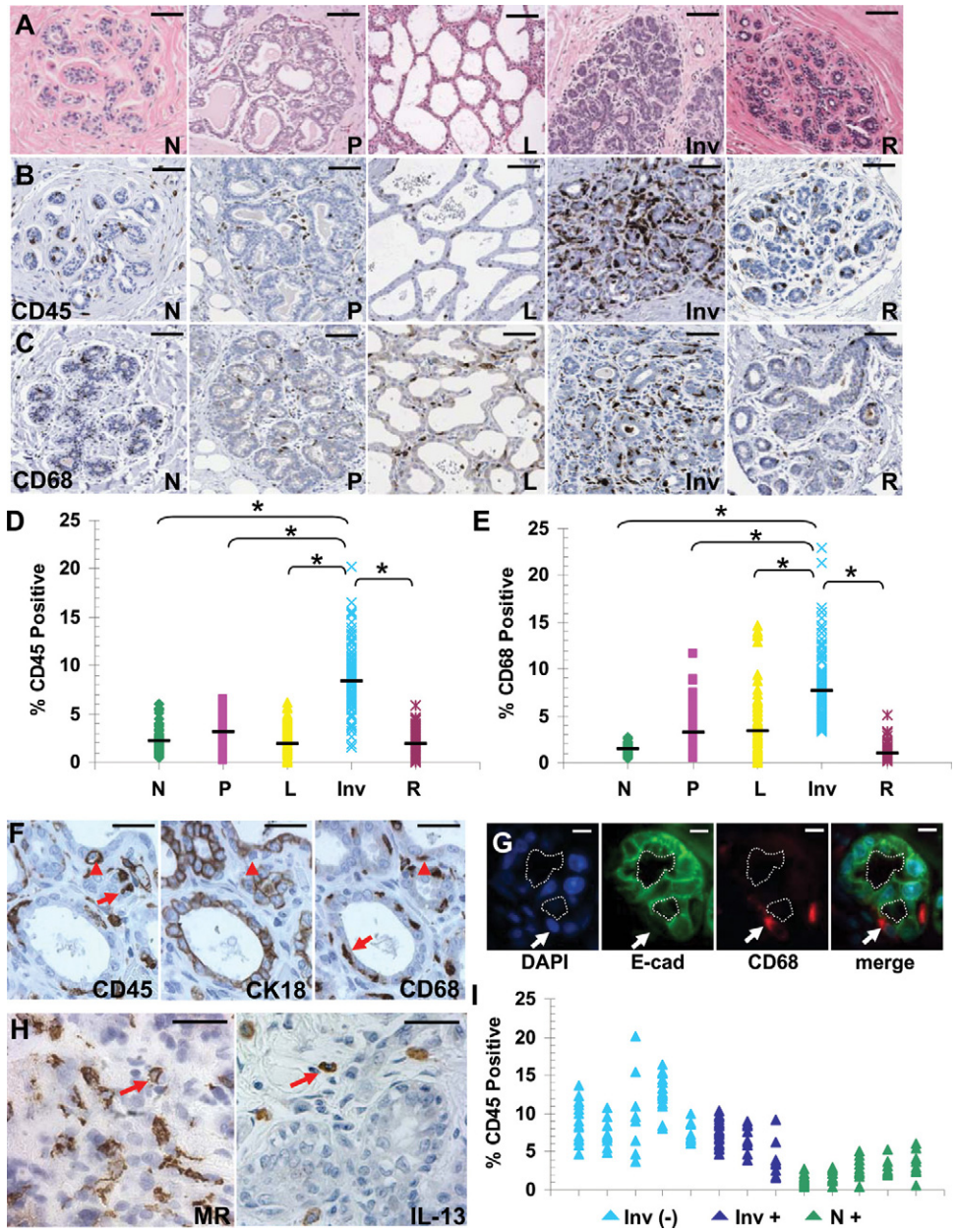

Figure 3. Characterization of postpartum lobule involution in human breast tissue. **A:** H&E-stained breast biopsy tissues from developmental stages representative of nulliparous (N), pregnant (P), lactation (L), involution (I), and regressed (R); scale bar represents 100 microns. Tissue sections Stained by IHC for: **B:** CD45, scale bar represents 100 microns. **C:** CD68, scale bar represents 100 microns. **D:** Quantification of CD45 staining as described in *Materials and Methods* section. Number (n) of cases for each developmental stage: nulliparous $n = 5$, pregnant $n = 8$, lactation $n = 11$, involution $n = 8$, regressed $n = 10$, * different from involution, $P < 0.0001$, Tukey–Kramer Multiple Comparisons Test. Black bars indicate average CD45 stain signal values for each developmental stage. **E:** Quantification of CD68 staining. Number (n) of cases for each developmental stage: nulliparous $n = 6$, pregnant $n = 9$, lactation $n = 9$, involution $n = 8$, regressed $n = 8$, * different from involution, $P < 0.0001$, Tukey–Kramer Multiple Comparisons Test. Black bars indicate average CD68 stain signal values for each developmental stage. **F:** Serial sections of human involuting breast biopsy tissue stained by IHC for CD45 (monocytes), CK18 (epithelial cells), and CD68 (macrophages) to reveal multiple cell populations present in human breast tissue, **arrowheads** indicate cells that are CD45- *and* CD68-positive but CK18-negative, **arrows** indicate cells that are either CD45-positive *or* CD68-negative and CK18-negative, scale bar represents 50 microns. **G:** Dual fluorescent staining of human involuting breast biopsy tissue using E-cadherin (green) to identify mammary epithelial cells and CD68 (red) to identify macrophages (**arrow**). Nuclei are stained blue with DAPI, the dotted line indicates the acinar lumen, scale bar represents 10 microns. **H:** Human involuting breast biopsy tissue stained by IHC for Macrophage Mannose Receptor (**arrow**) and M2 cytokine IL-13 (**arrow**), scale bar represents 50 microns. **I:** Involution (Inv) and nulliparous (N) cases from CD45 quantitation separated based on presence (+), or absence (−), of cancer in tissues examined.

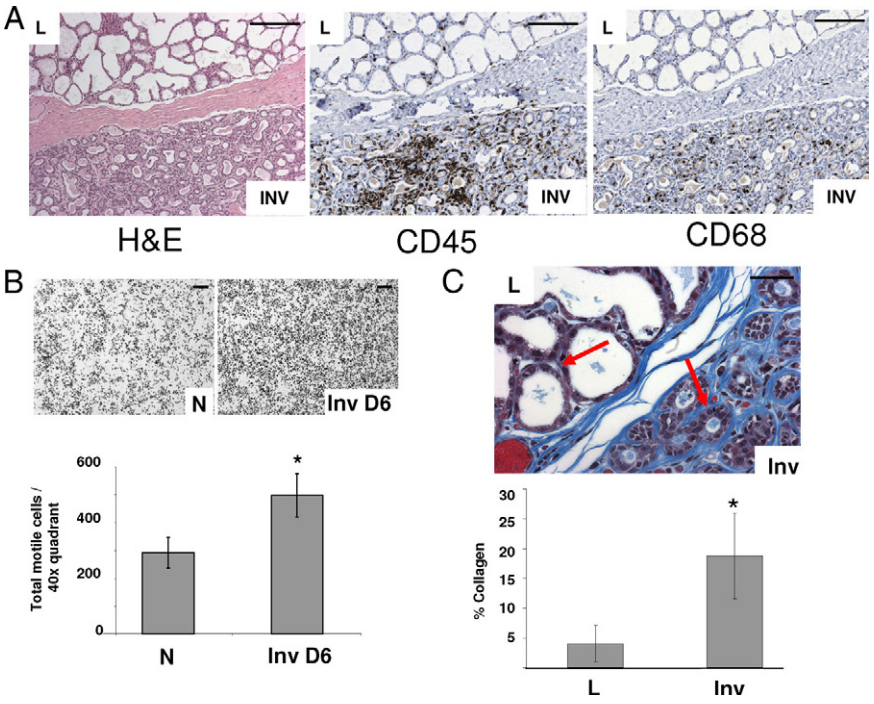

Figure 4. Immune cells are recruited to involuting lobules in part by fibrillar collagen. **A:** Human breast biopsy tissue with both lactating (**upper lobules**) and involuting (**lower lobules**) stained by H&E (**left panel**) and IHC for CD45 (**middle panel**) and CD68 (**right panel**) showing CD45 and CD68 specifically elevated in involuting lobules; scale bars represent 200 microns. **B:** Mammary ECM isolated from nulliparous (N) or involution day 6 (Inv D6) rats and used as chemoattractant for J774 mouse macrophages shows increased chemotaxis toward involution matrix (**upper panels**); scale bars represent 200 microns. Quantification of transwell filter data, chemotaxis toward involution matrix is increased compared with nulliparous matrix, three wells per condition, four quadrants per well, $n = 12$, $^*P = 0.0002$, unpaired t test. **C:** Human lactating/involuting breast biopsy tissue stained by Masson's trichrome method and individual lobules ($n = 77$ for lactation and $n = 70$ for involution) from four cases, scale bar represents 50 microns. **Arrows** indicate areas where collagen staining (blue) is evident. Images quantitated for percent composition of intralobular collagen, $^*P < 0.0001$, unpaired t test.

Gradual Weaning Reveals Collagen Rich Microenvironment in Involuting Lobules

Macrophages may be recruited to the involuting breast due to systemic events or alternatively in response to changes occurring locally within the involuting lobules. If systemic influences are responsible, then macrophage density would be anticipated to be uniform throughout the involuting breast. Conversely, if local or tissue microenvironment changes are responsible for recruitment, then it would be anticipated that macrophage recruitment would be heterogeneous. Evidence supporting local changes in the involuting gland as being responsible for recruitment was obtained through analyses of breast tissue from women who were gradually weaning at the time of tissue collection. In these specimens, individual lactating lobules were frequently found adjacent to actively involuting lobules (Figure 4A, left panel). Only the actively involuting lobules stained strongly for CD45- and CD68-positive cells (Figure 4A, middle and right panels, respectively). These results indicate that CD45-positive immune cells in general, and CD68-positive M2 macrophages specifically, are recruited to the involuting mammary gland as a result of specific changes within the involuting lobules.

Collagen as an ECM Mediator of Macrophage Recruitment

Several ECM fragments have demonstrated chemotactic activity for immune cells,[63] suggesting that changes in ECM specific to involuting lobules may account for macrophage influx. Consistent with these observations, mammary ECM biochemically extracted from involuting rat mammary glands was found to attract murine macrophages significantly more than nulliparous mammary ECM in transwell filter assays (Figure 4B, upper panel). One ECM protein that may be responsible for this recruitment is collagen I, as collagen I mRNA levels increase coincident with macrophage number during early stages of mammary involution in the mouse.[18] To determine whether collagen protein expression increases in involuting lobules in a pattern consistent with macrophage influx, human breast tissue collagen was stained blue using Masson's trichrome stain. Increased levels of collagen specific to involuting lobules were apparent when compared with the amount of staining observed in adjacent lactating lobules (Figure 4C, upper panel, arrows). These observations were confirmed by quantification of collagen stain intensity in individual lobules using the computer assisted histology quantitation program described above (Figure 4C, lower panel). This pattern of collagen accumulation identifies collagen as having a potential role in macrophage recruitment during involution.

To determine the timing of collagen increase during involution we returned to the rat model because tissue obtained at specific timepoints after weaning is essentially unavailable in women. Mammary tissue sections obtained from rats across the pregnancy, lactation, involution cycle were stained for fibrillar collagen using picrosirius red stain. Representative images demonstrate increased collagen accumulation both within and around (intra- and interlobular) involuting lobules when compared with virgin, pregnant, and lactating lobules (Figure 5A). Representative images of stained lactating and involuting glands are shown in Figure 5B. The increase in collagen around individual involuting lobules is clearly evident when the red picro-sirius signal is converted to a white signal and isolated onto a black background (Figure 5C). Quantitation of these images, with collagen lev-

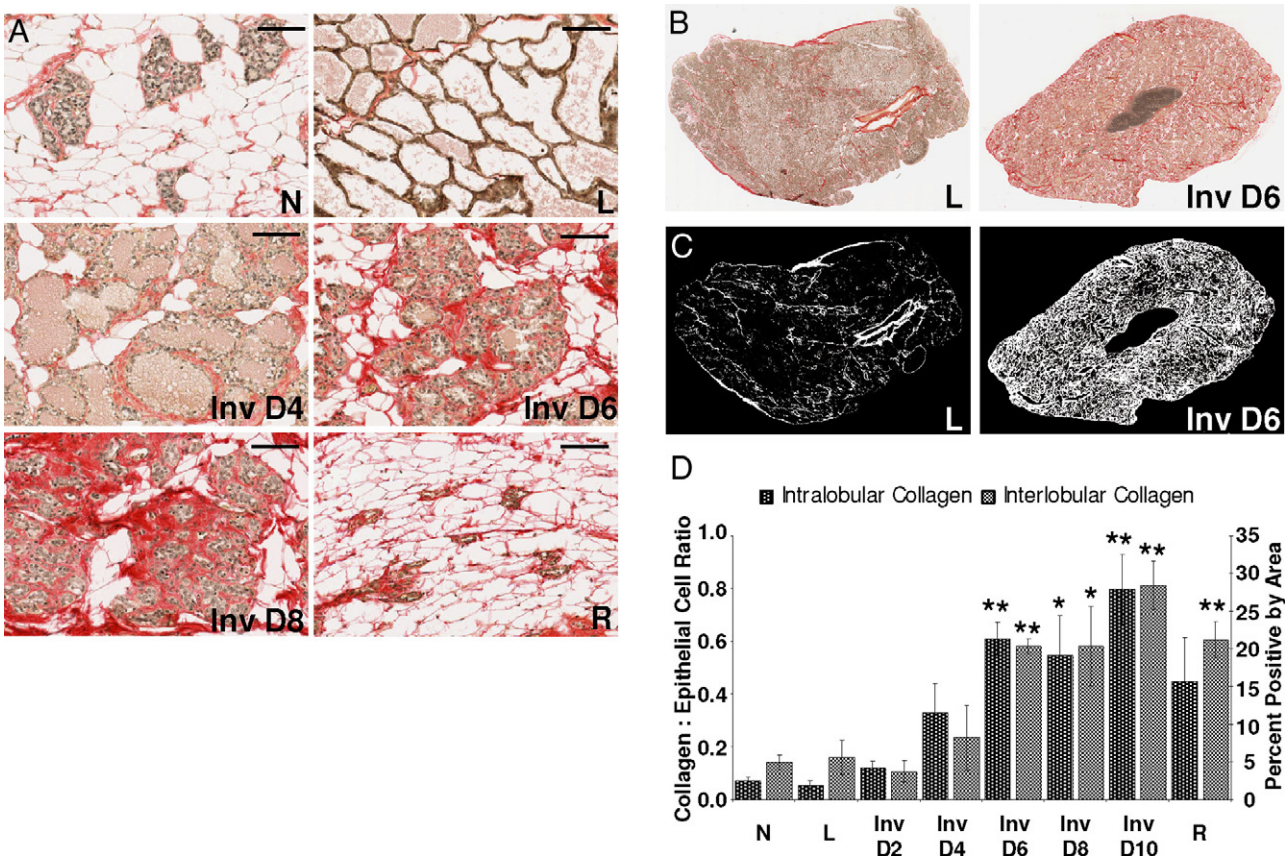

Figure 5. Intra- and extra-lobular collagen content increases during mammary involution. **A:** Picro-sirius red stain for collagen in rat mammary tissue; N indicates nulliparous; P, pregnant; L, lactation; Inv D, involution day; R, regressed; scale bars represent 100 microns. **B:** Whole section images of picro-sirius red collagen stain with brown nuclei. **C:** Images in **B** with collagen signal converted to white and noncollagen converted to black. **D:** Quantification of intralobular collagen (**left axis**) and interlobular collagen (**right axis**) ($n = 3$ rats per reproductive stage, $^{*}P < 0.05$, $^{**}P \leq 0.005$ compared with N, unpaired t test).

els normalized to epithelial content, demonstrates that both intra- and interlobular stromal collagen accumulate mid-involution and further increase through involution day 10 (Figure 5D). Whereas peak macrophage influx corresponds with high collagen levels, data from Figure 2B shows that macrophage number begins to increase as early as two days postweaning (Inv D2), which precedes the measurable increase in collagen observed at involution D4. However, we also show that levels of another known macrophage chemoattractant, MCP-1, rise around involution day 2, and may contribute to this earlier influx of macrophages (Figure 1D).

Collagen I peptides have been shown to be highly chemotactic for immune cells.[64] Thus, we determined whether the collagen deposited during involution is also proteolyzed. In accord with previously published results, in the rat we found that MMP-2 and MMP-9 activities were upregulated during mammary involution at days 4 to 6 (Figure 6A).[16,49] Both MMP-2 and MMP-9 are known to cleave collagen I.[16,49] Consistent with this elevated MMP activity, collagen I proteolysis was detected as early as four days postweaning in ECM isolated from the involuting gland (Figure 6B). To evaluate this potential interaction in an *in vitro* model, non fibrillar denatured collagen (gelatin) was used as a chemoattractant in a transwell filter chemotaxis assay. Murine macrophages showed significantly greater motility toward nonfibrillar collagen than fibrillar collagen or control sera (Figure 6C). Thus, elevated levels of partially proteolyzed nonfibrillar collagen may be one component of the ECM present in the involuting mammary gland that is chemotactic for macrophages. Together, these data suggest in the rat that early MCP-1 expression recruits macrophages at day two of involution and that collagen accumulation and proteolysis occurring during days 4 through 6 of involution, when tissue remodeling is at its peak, contribute to the recruitment of additional macrophages, whose levels peak at involution day 6 and day 8.

Discussion

We have shown an immune cell component that is inherent to the normal physiological process of postpartum mammary involution in rats, mice, and women, which resolves on completion of mammary involution. A high percentage of these immune cells are macrophages, which appear to be specifically recruited to the involution microenvironment because they are largely absent in adjacent lactational lobules in human breast tissue. The majority of macrophages present during postlactational involution in all three species exhibit an M2 phenotype.

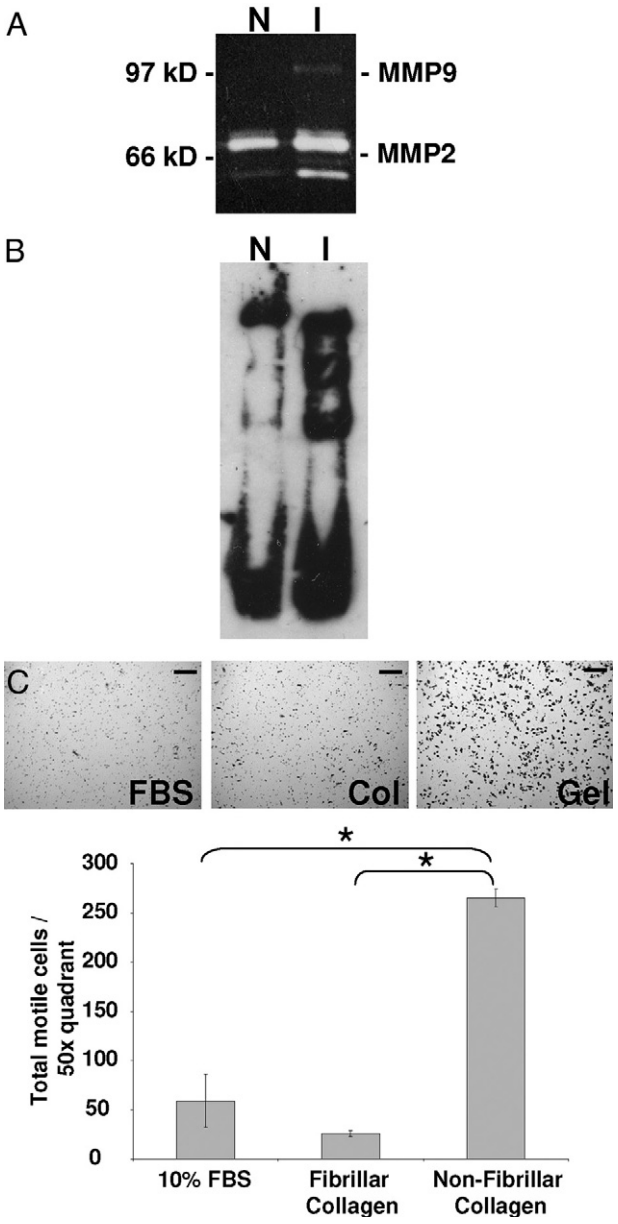

Figure 6. Increased MMP activities and proteolyzed collagen seen during mammary involution may account for macrophage chemotaxis observed *in vivo*. **A:** Gelatin zymogen assay using mammary tissue lysates from nulliparous (N) or involution days 4 to 6 (I) rats depicts increased MMP-9 and activity MMP-2 in involuting mammary tissue. **B:** Western blot for collagen-1 using mammary ECM from nulliparous (N) or involution days 4 to 6 (I) rats shows partial proteolysis of collagen I during involution. **C:** 10% FBS, fibrillar collagen, or nonfibrillar collagen (gelatin) used as chemoattractant for J774 mouse macrophages and quantified per ×50 quadrant; scale bars represent 100 microns, $n = 3$, $^*P < 0.002$, unpaired t test.

M2 macrophages have been shown to have cytokine profiles and functional phenotypes similar to TAMs,[34] and TAMs correlate with negative outcomes in breast cancer patients.[40,65] The presence of M2 macrophages during postlactational involution may provide insight into mechanisms that account for the poor prognosis of women diagnosed with PABC. In a recent literature review on the epidemiology of PABC, two distinct subtypes were defined.[6] Subtype 1, or breast cancer diagnosed during pregnancy, carries a prognosis similar to non-PABC when matched for mother's age, tumor stage, and aggressiveness of treatment. Subtype 2, breast cancer diagnosed within five years of a completed pregnancy, is linked with poorer prognosis when matched for these same parameters. For example, in the studies examined, PABC patients diagnosed after pregnancy (subtype 2) had lower survival percentages, ranging from 6.5% to 64.9% compared with patients diagnosed during pregnancy (subtype 1) whose percent survival ranged from 56% to 72%. Non-PABC patients had the best prognosis with percent survival ranging from 64.8% to 97%.[6] We hypothesize that the major differences in survival rates observed between the two PABC subtypes may be attributable to exposure of the tumor cells to the involution microenvironment. The involution microenvironment, with its wound healing attributes including the M2 macrophage phenotype, is likely to accelerate progression of breast cancers in the postpartum setting.[66–71]

Whether M2 macrophages in the involuting gland have the ability to promote breast cancer is not yet known. However, based on the role of TAMs in breast cancer progression for women of all ages, it is anticipated that involution-associated M2 macrophages contribute in some manner to PABC. For example, decreased relapse-free and overall survival is associated with TAM infiltration into breast tumors,[36] and metastasis occurs earlier in patients with increased TAM number.[36,37] Further, in a meta analysis, 12 of 15 separate studies comparing TAMs and cancer prognosis showed negative outcomes correlating with increased TAM accumulation.[65] Supporting evidence for this interaction has been compiled from genetic studies in the rodent. This work used polyoma middle-T oncoprotein (PyMT) expression driven by the mammary epithelial cell specific mouse mammary tumor virus promoter (MMTV) in combination with various genetic manipulations of CSF-1. Ablation of cells expressing CSF-1, which was highly selective for loss of macrophages, demonstrated that CSF-1–responsive cells were necessary for the angiogenic switch that occurs during tumor progression and lung metastasis. Conversely, overexpression of CSF-1 in this model results in an increased number of macrophages, earlier angiogenesis, and significantly more lung metastasis.[33,72] Identifying the molecular link between involution, M2 macrophages, and tumor progression is of importance and Stat3, a transcription factor mediating wound healing, inflammation, and immunosuppression in the tumor microenvironment, is a potential candidate. Stat3 expression is specifically upregulated early in involution, where it has been implicated in inducing an acute phase response.[23,24] Recently, an *in vivo* analysis demonstrated a requirement for Stat3 in mammary tumor metastasis and implicated inflammatory pathways driven by the acute phase response in the metastasis process.[73] Together, these results emphasize the role of macrophages in tumor cell escape from the primary tumor and successful seeding at distant locations and identify endogenous Stat3 upregulation as a possible mediator of these events.

Our data suggest that macrophages are actively recruited to the involuting mammary gland, and the mech-

anisms responsible for this recruitment are of great interest. We show that ECM isolated from involuting rat mammary glands is chemotactic for murine macrophages *in vitro*, indicating a possible ECM mediator of macrophage recruitment. Several ECM proteins, including collagens, are chemotactic to macrophages.[74–76] We have revealed increased deposition of collagen in actively involuting human breast lobules implicating collagen as a mediator of macrophage recruitment. A temporal analysis of collagen accumulation throughout the involution period in the rat model shows increased collagen levels as early as day 4 of involution. These data complement earlier studies that demonstrated an increase in procollagen I and III transcripts at two days post weaning.[18] We demonstrate partial proteolysis of collagen I in the involuting rat mammary gland and increased macrophage cell chemotaxis toward denatured collagen *in vitro*. These results compliment other data recently published by our lab where mammary gland collagen proteolysis was suppressed by treatment with the breast cancer therapeutic drug tamoxifen. Under these conditions, mammary macrophage recruitment was concurrently reduced.[77] It is of interest to note that several other ECM proteins are also partially proteolyzed during involution, including fibronectin, laminin1, laminin 5, and entactin.[49,78] *In vitro*, macrophages are attracted to ECM fragments derived from these ECM proteins as well, implicating their proteolysis in macrophage recruitment during involution. As MCP-1, IL-4, and IL-13 have also been observed to act as macrophage chemoattractants[79–81] and increase during the involution period in the rat mammary gland (Figures 1D and 2, C and D), the involution microenvironment is primed for macrophage accumulation.

Although collagen may play a role in tumor promotion through its recruitment of macrophages to the involuting gland, collagen deposition and proteolysis are likely to promote invasion and metastasis by other mechanisms as well. For example, proteolytic exposure of a cryptic site within collagen IV can promote tumor angiogenesis[82] and metastasis[83] *in vivo*. Further, nonfibrillar collagen I releases melanoma cells from cell-cycle–induced proliferative arrest.[84] Additional evidence implicating collagen in tumor cell progression was obtained using a bitransgenic mouse tumor model designed to study the role of breast density on tumorigenesis. These mice carry the MMTV-PyMT transgene to initiate tumorigenesis and have mutations in the MMP cleavage site for collagen I, and as a result accumulate excess stromal collagen during mammary gland development.[85] These mice showed increased mammary tumor formation, progression to invasion, and increased lung metastasis. Further, local tumor cell invasion was facilitated by reorganization of stromal collagen in the collagen dense mammary tissue, and epithelial cells isolated from tumors that arose in the collagen dense stroma were more migratory in transwell filter assays.[85] It can be postulated that the abundant collagen present in the normal involuting mammary gland may similarly serve to alter the tumorigenic phenotype of premalignant and malignant tumor cells.

Another large body of research focuses on the role of collagen stiffness in mammary tumor progression and metastasis.[86] Involution is characterized by extensive remodeling of the ECM and matrix stiffening,[87,88] data consistent with our observations of increased collagen deposition during involution. When collagen is progressively stiffened, *in vitro* breast tumor cell growth is stimulated, cell–cell junctions are compromised, and cell invasion is enhanced through elevated ERK and Rho-kinase activities.[86,89] Similarly, increased stromal collagen may directly influence mammary fibroblasts, which in turn influence the mammary epithelium through numerous paracrine signal transduction pathways including TGF-β, EGF, FGF, IGF-1, and HGF.[90–96] Consistent with these observations, dense breast tissue, which is thought to have high collagen content, is associated with increased local[97] and circulating levels of IGF-1.[98,99] Additionally, in animal models, migrating mammary epithelial tumor cells are observed to migrate along linear bundles of collagen fibers found adjacent to blood vessels,[85,100,101] indicating that stiff collagen fibers may provide a favorable route for metastatic cell migration. Finally, tumor cell–derived ECM shows increased lysyl-oxidase–dependant collagen crosslinking,[102,103] and nonlinear optical imaging approaches have revealed that local invasion of breast tumors can be facilitated by collagen reorganization induced by such crosslinking.[85] The question of whether the collagens deposited during involution are similarly crosslinked and/or reorganized remains to be determined.

Based on the numerous protumorigenic attributes of collagen, it is of interest to note that although the increase in macrophages that we observe during involution is largely resolved when the gland reaches a fully regressed state, collagen levels remained high in the fully regressed rat mammary gland (Figure 5D). Preliminary data also indicate that the fully regressed human gland carries increased collagen content when compared with nulliparous tissue (data not shown). Because it is widely accepted that fully regressed rat and human mammary tissues are protected from transformation by parity,[104] and ECM isolated from fully regressed rat mammary glands has been demonstrated to have tumor suppressive attributes in cell culture assays,[49] the elevated collagen content of the fully involuted gland appears paradoxical. Given this apparent paradox, it is important to emphasize that although the amount of collagen deposition in the involuting and fully regressed glands are both increased over nulliparous levels, the tumor promoting effects of collagen are based not simply on abundance but also type, organizational state, proteolysis, and extent of crosslinking. The question of whether collagen differs between the actively involuting mammary gland and the fully regressed gland remains an interesting but unanswered question.

In summary, our studies show that the tissue microenvironment of the postpartum involuting mammary gland is characterized by alternatively activated, M2-type macrophages, recruited in part by deposition and proteolysis of collagen I. M2 macrophages, collagen I deposition, and collagen proteolysis are tumor promotional in other settings. We propose that these involution-induced changes

in the microenvironment are partially responsible for the poor prognosis of breast cancers diagnosed in women shortly after a completed pregnancy. Future studies are required to determine the roles of M2 macrophages in normal postpartum breast involution and in the poor prognosis of PABC subtype 2. The ultimate goal is to determine whether the functional plasticity of macrophages can be exploited to prevent progression of PABC subtype 2 in women at high risk for metastasis.

Acknowledgments

We acknowledge K. Pat Bell for extensive IHC protocol development and staining, Holly Martinson and Neena Gupta for help with histological staining and quantification in the rodent studies, Ori Maller for assistance with chemotaxis assays, Susan Edgerton for tissue acquisition logistics, and Steve Anderson and Heide Ford for critical review of the manuscript. We also thank the patients for their contribution to this research.

References

1. Lambe M, Hsieh C, Trichopoulos D, Ekbom A, Pavia M, Adami HO: Transient increase in the risk of breast cancer after giving birth. N Engl J Med 1994, 331:5–9
2. Chie WC, Hsieh C, Newcomb PA, Longnecker MP, Mittendorf R, Greenberg ER, Clapp RW, Burke KP, Titus-Ernstoff L, Trentham-Dietz A, MacMahon B: Age at any full-term pregnancy and breast cancer risk. Am J Epidemiol 2000, 151:715–722
3. Albrektsen G, Heuch I, Hansen S, Kvale G: Breast cancer risk by age at birth, time since birth and time intervals between births: exploring interaction effects. Br J Cancer 2005, 92:167–175
4. Liu Q, Wuu J, Lambe M, Hsieh SF, Ekbom A, Hsieh CC: Transient increase in breast cancer risk after giving birth: postpartum period with the highest risk (Sweden). Cancer Causes Control 2002, 13:299–305
5. Schedin P: Pregnancy-associated breast cancer and metastasis. Nat Rev Cancer 2006, 6:281–291
6. Lyons TR, Schedin PJ, Borges VF: Pregnancy and breast cancer: when they collide. J Mammary Gland Biol Neoplasia 2009, 14:87–98
7. Stensheim H, Moller B, van Dijk T, Fossa SD: Cause-specific survival for women diagnosed with cancer during pregnancy or lactation: a registry-based cohort study. J Clin Oncol 2009, 27:45–51
8. Mathelin C, Annane K, Treisser A, Chenard MP, Tomasetto C, Bellocq JP, Rio MC: Pregnancy and post-partum breast cancer: a prospective study. Anticancer Res 2008, 28:2447–2452
9. Lethaby AE, O'Neill MA, Mason BH, Holdaway IM, Harvey VJ: Overall survival from breast cancer in women pregnant or lactating at or after diagnosis. Auckland Breast Cancer Study Group. Int J Cancer 1996, 67:751–755
10. Rodriguez AO, Chew H, Cress R, Xing G, McElvy S, Danielsen B, Smith L: Evidence of poorer survival in pregnancy-associated breast cancer. Obstet Gynecol 2008, 112:71–78
11. Daling JR, Malone KE, Doody DR, Anderson BO, Porter PL: The relation of reproductive factors to mortality from breast cancer. Cancer Epidemiol Biomarkers Prev 2002, 11:235–241
12. Bladstrom A, Anderson H, Olsson H: Worse survival in breast cancer among women with recent childbirth: results from a Swedish population-based register study. Clin Breast Cancer 2003, 4:280–285
13. Whiteman MK, Hillis SD, Curtis KM, McDonald JA, Wingo PA, Marchbanks PA: Reproductive history and mortality after breast cancer diagnosis. Obstet Gynecol 2004, 104:146–154
14. Phillips KA, Milne RL, West DW, Goodwin PJ, Giles GG, Chang ET, Figueiredo JC, Friedlander ML, Keegan TH, Glendon G, Apicella C, O'Malley FP, Southey MC, Andrulis IL, John EM, Hopper JL: Prediagnosis reproductive factors and all-cause mortality for women with breast cancer in the breast cancer family registry. Cancer Epidemiol Biomarkers Prev 2009, 18:1792–1797
15. Phillips KA, Milne RL, Friedlander ML, Jenkins MA, McCredie MR, Giles GG, Hopper JL: Prognosis of premenopausal breast cancer and childbirth prior to diagnosis. J Clin Oncol 2004, 22:699–705
16. McDaniel SM, Rumer KK, Biroc SL, Metz RP, Singh M, Porter W, Schedin P: Remodeling of the Mammary Microenvironment after Lactation Promotes Breast Tumor Cell Metastasis. Am J Pathol 2006, 168:363–366
17. Bemis LT, Schedin P: Reproductive state of rat mammary gland stroma modulates human breast cancer cell migration and invasion. Cancer Res 2000, 60:3414–3418
18. Schedin P, O'Brien J, Rudolph M, Stein T, Borges V: Microenvironment of the involuting mammary gland mediates mammary cancer progression. J Mammary Gland Biol Neoplasia 2007, 12:71–82
19. Walker NI, Bennett RE, Kerr JF: Cell death by apoptosis during involution of the lactating breast in mice and rats. Am J Anat 1989, 185:19–32
20. Strange R, Li F, Saurer S, Burkhardt A, Friis RR: Apoptotic cell death and tissue remodelling during mouse mammary gland involution. Development 1992, 115:49–58
21. Alexander CM, Selvarajan S, Mudgett J, Werb Z: Stromelysin-1 regulates adipogenesis during mammary gland involution. J Cell Biol 2001, 152:693–703
22. Schenk S, Hintermann E, Bilban M, Koshikawa N, Hojilla C, Khokha R, Quaranta V: Binding to EGF receptor of a laminin-5 EGF-like fragment liberated during MMP-dependent mammary gland involution. J Cell Biol 2003, 161:197–209
23. Stein T, Morris JS, Davies CR, Weber-Hall SJ, Duffy MA, Heath VJ, Bell AK, Ferrier RK, Sandilands GP, Gusterson BA: Involution of the mouse mammary gland is associated with an immune cascade and an acute-phase response, involving LBP, CD14, and STAT3. Breast Cancer Res 2004, 6:R75–R91
24. Clarkson RW, Wayland MT, Lee J, Freeman T, Watson CJ: Gene expression profiling of mammary gland development reveals putative roles for death receptors and immune mediators in post-lactational regression. Breast Cancer Res 2004, 6:R92–R109
25. Schedin P, Strange R, Mitrenga T, Wolfe P, Kaeck M: Fibronectin fragments induce MMP activity in mouse mammary epithelial cells: evidence for a role in mammary tissue remodeling. J Cell Sci 2000, 113 (Pt 5):795–806
26. Mantovani A, Sica A, Sozzani S, Allavena P, Vecchi A, Locati M: The chemokine system in diverse forms of macrophage activation and polarization. Trends Immunol 2004, 25:677–686
27. Van Ginderachter JA, Movahedi K, Hassanzadeh Ghassabeh G, Meerschaut S, Beschin A, Raes G, De Baetselier P: Classical and alternative activation of mononuclear phagocytes: picking the best of both worlds for tumor promotion. Immunobiology 2006, 211: 487–501
28. Gordon S: Alternative activation of macrophages. Nat Rev Immunol 2003, 3:23–35
29. Meneghin A, Hogaboam CM: Infectious disease, the innate immune response, and fibrosis. J Clin Invest 2007, 117:530–538
30. Stout RD, Watkins SK, Suttles J: Functional plasticity of macrophages: in situ reprogramming of tumor-associated macrophages. J Leukoc Biol 2009, 86:1105–1109
31. Mantovani A, Sozzani S, Locati M, Allavena P, Sica A: Macrophage polarization: tumor-associated macrophages as a paradigm for polarized M2 mononuclear phagocytes. Trends Immunol 2002, 23: 549–555
32. Paulus P, Stanley ER, Schafer R, Abraham D, Aharinejad S: Colony-stimulating factor-1 antibody reverses chemoresistance in human MCF-7 breast cancer xenografts. Cancer Res 2006, 66:4349–4356
33. Lin EY, Nguyen AV, Russell RG, Pollard JW: Colony-stimulating factor 1 promotes progression of mammary tumors to malignancy. J Exp Med 2001, 193:727–740
34. Sica A, Schioppa T, Mantovani A, Allavena P: Tumour-associated macrophages are a distinct M2 polarised population promoting tumour progression: potential targets of anti-cancer therapy. Eur J Cancer 2006, 42:717–727
35. Ueno T, Toi M, Saji H, Muta M, Bando H, Kuroi K, Koike M, Inadera H, Matsushima K: Significance of macrophage chemoattractant protein-1 in macrophage recruitment, angiogenesis, and survival in human breast cancer. Clin Cancer Res 2000, 6:3282–3289

36. Leek RD, Lewis CE, Whitehouse R, Greenall M, Clarke J, Harris AL: Association of macrophage infiltration with angiogenesis and prognosis in invasive breast carcinoma. Cancer Res 1996, 56: 4625–4629
37. Tsutsui S, Yasuda K, Suzuki K, Tahara K, Higashi H, Era S: Macrophage infiltration and its prognostic implications in breast cancer: the relationship with VEGF expression and microvessel density. Oncol Rep 2005, 14:425–431
38. Kacinski BM, Scata KA, Carter D, Yee LD, Sapi E, King BL, Chambers SK, Jones MA, Pirro MH, Stanley ER: FMS (CSF-1 receptor) and CSF-1 transcripts and protein are expressed by human breast carcinomas in vivo and in vitro. Oncogene 1991, 6:941–952
39. McDermott RS, Deneux L, Mosseri V, Vedrenne J, Clough K, Fourquet A, Rodriguez J, Cosset JM, Sastre X, Beuzeboc P, Pouillart P, Scholl SM: Circulating macrophage colony stimulating factor as a marker of tumour progression. Eur Cytokine Netw 2002, 13:121–127
40. O'Brien J, Schedin P: Macrophages in breast cancer: do involution macrophages account for the poor prognosis of pregnancy-associated breast cancer? J Mammary Gland Biol Neoplasia 2009, 14:145–157
41. Schedin P, Mitrenga T, Kaeck M: Estrous cycle regulation of mammary epithelial cell proliferation, differentiation, and death in the Sprague-Dawley rat: a model for investigating the role of estrous cycling in mammary carcinogenesis. J Mammary Gland Biol Neoplasia 2000, 5:211–225
42. Lopez-De Leon A, Rojkind M: A simple micromethod for collagen and total protein determination in formalin-fixed paraffin-embedded sections. J Histochem Cytochem 1985, 33:737–743
43. Slattery ML, Sweeney C, Edwards S, Herrick J, Baumgartner K, Wolff R, Murtaugh M, Baumgartner R, Giuliano A, Byers T: Body size, weight change, fat distribution and breast cancer risk in Hispanic and non-Hispanic white women. Breast Cancer Res Treat 2007, 102:85–101
44. Werahera PN, Miller GJ, Torkko K, Crawford ED, Stewart JS, Deantoni EP, Miller HL, Lucia MS: Biomorphometric analysis of human prostatic carcinoma by using three-dimensional computer models. Hum Pathol 2004, 35:798–807
45. Kawata N, Miller GJ, Crawford ED, Torkko KC, Stewart JS, Lucia MS, Miller HL, Hirano D, Werahera PN: Laterally directed biopsies detect more clinically threatening prostate cancer: computer simulated results. Prostate 2003, 57:118–128
46. Rasband W: Image J. National Institutes of Health, Bethesda MD, 1997–2008.
47. Kleinman HK, McGarvey ML, Hassell JR, Star VL, Cannon FB, Laurie GW, Martin GR: Basement membrane complexes with biological activity. Biochemistry 1986, 25:312–318
48. Hahm HA, Ip MM: Primary culture of normal rat mammary epithelial cells within a basement membrane matrix. I Regulation of proliferation by hormones and growth factors. In Vitro Cell Dev Biol 1990, 26:791–802
49. Schedin P, Mitrenga T, McDaniel S, Kaeck M: Mammary ECM composition and function are altered by reproductive state. Mol Carcinog 2004, 41:207–220
50. Monks J, Smith-Steinhart C, Kruk ER, Fadok VA, Henson PM: Epithelial cells remove apoptotic epithelial cells during post-lactation involution of the mouse mammary gland. Biol Reprod 2008, 78:586–594
51. Martinez-Pomares L, Platt N, McKnight AJ, da Silva RP, Gordon S: Macrophage membrane molecules: markers of tissue differentiation and heterogeneity. Immunobiology 1996, 195:407–416
52. Stanley ER, Berg KL, Einstein DB, Lee PS, Pixley FJ, Wang Y, Yeung YG: Biology and action of colony–stimulating factor-1. Mol Reprod Dev 1997, 46:4–10
53. Rabinowitz SS, Gordon S: Macrosialin, a macrophage-restricted membrane sialoprotein differentially glycosylated in response to inflammatory stimuli. J Exp Med 1991, 174:827–836
54. Masaki T, Chow F, Nikolic-Paterson DJ, Atkins RC, Tesch GH: Heterogeneity of antigen expression explains controversy over glomerular macrophage accumulation in mouse glomerulonephritis. Nephrol Dial Transplant 2003, 18:178–181
55. McKnight AJ, Gordon S: Membrane molecules as differentiation antigens of murine macrophages. Adv Immunol 1998, 68:271–314
56. Pillai MM, Hayes B, Torok-Storb B: Inducible transgenes under the control of the hCD68 promoter identifies mouse macrophages with a distribution that differs from the F4/80 and CSF-1R expressing populations. Exp Hematol 2009, 37:1387–1392
57. Richert MM, Schwertfeger KL, Ryder JW, Anderson SM: An atlas of mouse mammary gland development. J Mammary Gland Biol Neoplasia 2000, 5:227–241
58. Singh M, McGinley JN, Thompson HJ: A comparison of the histopathology of premalignant and malignant mammary gland lesions induced in sexually immature rats with those occurring in the human. Lab Invest 2000, 80:221–231
59. Russo J, Gusterson BA, Rogers AE, Russo IH, Wellings SR, van Zwieten MJ: Comparative study of human and rat mammary tumorigenesis. Lab Invest 1990, 62:244–278
60. Cardiff RD, Wellings SR: The comparative pathology of human and mouse mammary glands. J Mammary Gland Biol Neoplasia 1999, 4:105–122
61. Hermiston ML, Xu Z, Weiss A: CD45: a critical regulator of signaling thresholds in immune cells. Annu Rev Immunol 2003, 21:107–137
62. Noorman F, Braat EA, Barrett-Bergshoeff M, Barbe E, van Leeuwen A, Lindeman J, Rijken DC: Monoclonal antibodies against the human mannose receptor as a specific marker in flow cytometry and immunohistochemistry for macrophages. J Leukoc Biol 1997, 61: 63–72
63. Adair-Kirk TL, Senior RM: Fragments of extracellular matrix as mediators of inflammation. Int J Biochem Cell Biol 2008, 40:1101–1110
64. Weathington NM, van Houwelingen AH, Noerager BD, Jackson PL, Kraneveld AD, Galin FS, Folkerts G, Nijkamp FP, Blalock JE: A novel peptide CXCR ligand derived from extracellular matrix degradation during airway inflammation. Nat Med 2006, 12:317–323
65. Bingle L, Brown NJ, Lewis CE: The role of tumour-associated macrophages in tumour progression: implications for new anticancer therapies. J Pathol 2002, 196:254–265
66. Mantovani A, Allavena P, Sica A, Balkwill F: Cancer-related inflammation. Nature 2008, 454:436–444
67. Coussens LM, Werb Z: Inflammation and cancer. Nature 2002, 420:860–867
68. Dvorak HF: Tumors: wounds that do not heal. Similarities between tumor stroma generation and wound healing. N Engl J Med 1986, 315:1650–1659
69. Tlsty TD: Stromal cells can contribute oncogenic signals. Semin Cancer Biol 2001, 11:97–104
70. Schedin P, Elias A: Multistep tumorigenesis and the microenvironment. Breast Cancer Res 2004, 6:93–101
71. Orimo A, Weinberg RA: Stromal fibroblasts in cancer: a novel tumor-promoting cell type. Cell Cycle 2006, 5:1597–1601
72. Lin EY, Li JF, Gnatovskiy L, Deng Y, Zhu L, Grzesik DA, Qian H, Xue XN, Pollard JW: Macrophages regulate the angiogenic switch in a mouse model of breast cancer. Cancer Res 2006, 66:11238–11246
73. Ranger JJ, Levy DE, Shahalizadeh S, Hallett M, Muller WJ: Identification of a Stat3-dependent transcription regulatory network involved in metastatic progression. Cancer Res 2009, 69:6823–6830
74. Adair-Kirk TL, Atkinson JJ, Broekelmann TJ, Doi M, Tryggvason K, Miner JH, Mecham RP, Senior RM: A site on laminin alpha 5. AQARSAASKVKVSMKF, induces inflammatory cell production of matrix metalloproteinase-9 and chemotaxis. J Immunol 2003, 171:398–406
75. Hance KA, Tataria M, Ziporin SJ, Lee JK, Thompson RW: Monocyte chemotactic activity in human abdominal aortic aneurysms: role of elastin degradation peptides and the 67-kD cell surface elastin receptor. J Vasc Surg 2002, 35:254–261
76. Guo G, Booms P, Halushka M, Dietz HC, Ney A, Stricker S, Hecht J, Mundlos S, Robinson PN: Induction of macrophage chemotaxis by aortic extracts of the mgR Marfan mouse model and a GxxPG-containing fibrillin-1 fragment. Circulation 2006, 114:1855–1862
77. Hattar R, Maller O, McDaniel S, Hansen KC, Hedman KJ, Lyons TR, Lucia S, Wilson RS Jr, Schedin P: Tamoxifen induces pleiotrophic changes in mammary stroma resulting in extracellular matrix that suppresses transformed phenotypes. Breast Cancer Res 2009, 11:R5
78. Alexander CM, Howard EW, Bissell MJ, Werb Z: Rescue of mammary epithelial cell apoptosis and entactin degradation by a tissue inhibitor of metalloproteinases-1 transgene. J Cell Biol 1996, 135: 1669–1677
79. Fujimoto H, Sangai T, Ishii G, Ikehara A, Nagashima T, Miyazaki M, Ochiai A: Stromal MCP-1 in mammary tumors induces tumor-associated macrophage infiltration and contributes to tumor progression. Int J Cancer 2009, 125:1276–1284

80. Hiester AA, Metcalf DR, Campbell PA: Interleukin-4 is chemotactic for mouse macrophages. Cell Immunol 1992, 139:72–80
81. Lebel-Binay S, Laguerre B, Quintin-Colonna F, Conjeaud H, Magazin M, Miloux B, Pecceu F, Caput D, Ferrara P, Fradelizi D: Experimental gene therapy of cancer using tumor cells engineered to secrete interleukin-13. Eur J Immunol 1995, 25:2340–2348
82. Xu J, Rodriguez D, Petitclerc E, Kim JJ, Hangai M, Moon YS, Davis GE, Brooks PC: Proteolytic exposure of a cryptic site within collagen type IV is required for angiogenesis and tumor growth in vivo. J Cell Biol 2001, 154:1069–1079
83. Roth JM, Caunt M, Cretu A, Akalu A, Policarpio D, Li X, Gagne P, Formenti S, Brooks PC: Inhibition of experimental metastasis by targeting the HUIV26 cryptic epitope in collagen. Am J Pathol 2006, 168:1576–1586
84. Wall SJ, Werner E, Werb Z, DeClerck YA: Discoidin domain receptor 2 mediates tumor cell cycle arrest induced by fibrillar collagen. J Biol Chem 2005, 280:40187–40194
85. Provenzano PP, Inman DR, Eliceiri KW, Knittel JG, Yan L, Rueden CT, White JG, Keely PJ: Collagen density promotes mammary tumor initiation and progression. BMC Med 2008, 6:11–25
86. Butcher DT, Alliston T, Weaver VM: A tense situation: forcing tumour progression. Nat Rev Cancer 2009, 9:108–122
87. Green KA, Lund LR: ECM degrading proteases and tissue remodelling in the mammary gland. Bioessays 2005, 27:894–903
88. Watson CJ: Post-lactational mammary gland regression: molecular basis and implications for breast cancer. Expert Rev Mol Med 2006, 8:1–15
89. Paszek MJ, Zahir N, Johnson KR, Lakins JN, Rozenberg GI, Gefen A, Reinhart-King CA, Margulies SS, Dembo M, Boettiger D, Hammer DA, Weaver VM: Tensional homeostasis and the malignant phenotype. Cancer Cell 2005, 8:241–254
90. Chung LW, Baseman A, Assikis V, Zhau HE: Molecular insights into prostate cancer progression: the missing link of tumor microenvironment. J Urol 2005, 173:10–20
91. De Wever O, Mareel M: Role of tissue stroma in cancer cell invasion. J Pathol 2003, 200:429–447
92. Condeelis J, Singer RH, Segall JE: The great escape: when cancer cells hijack the genes for chemotaxis and motility. Annu Rev Cell Dev Biol 2005, 21:695–718
93. Parr C, Watkins G, Mansel RE, Jiang WG: The hepatocyte growth factor regulatory factors in human breast cancer. Clin Cancer Res 2004, 10:202–211
94. Sachdev D, Yee D: The IGF system and breast cancer. Endocr Relat Cancer 2001, 8:197–209
95. Surmacz E: Function of the IGF-I receptor in breast cancer. J Mammary Gland Biol Neoplasia 2000, 5:95–105
96. Xian W, Schwertfeger KL, Vargo-Gogola T, Rosen JM: Pleiotropic effects of FGFR1 on cell proliferation, survival, and migration in a 3D mammary epithelial cell model. J Cell Biol 2005, 171:663–673
97. Guo YP, Martin LJ, Hanna W, Banerjee D, Miller N, Fishell E, Khokha R, Boyd NF: Growth factors and stromal matrix proteins associated with mammographic densities. Cancer Epidemiol Biomarkers Prev 2001, 10:243–248
98. Byrne C, Colditz GA, Willett WC, Speizer FE, Pollak M, Hankinson SE: Plasma insulin-like growth factor (IGF) I. IGF-binding protein 3, and mammographic density. Cancer Res 2000, 60:3744–3748
99. Boyd NF, Stone J, Martin LJ, Jong R, Fishell E, Yaffe M, Hammond G, Minkin S: The association of breast mitogens with mammographic densities. Br J Cancer 2002, 87:876–882
100. Ingman WV, Wyckoff J, Gouon-Evans V, Condeelis J, Pollard JW: Macrophages promote collagen fibrillogenesis around terminal end buds of the developing mammary gland. Dev Dyn 2006, 235:3222–3229
101. Wyckoff JB, Pinner SE, Gschmeissner S, Condeelis JS, Sahai E: ROCK- and myosin-dependent matrix deformation enables protease-independent tumor-cell invasion in vivo. Curr Biol 2006, 16:1515–1523
102. Payne SL, Hendrix MJ, Kirschmann DA: Paradoxical roles for lysyl oxidases in cancer–a prospect. J Cell Biochem 2007, 101:1338–1354
103. Rodriguez C, Rodriguez-Sinovas A, Martinez-Gonzalez J: Lysyl oxidase as a potential therapeutic target. Drug News Perspect 2008, 21:218–224
104. Medina D: Breast cancer: the protective effect of pregnancy. Clin Cancer Res 2004, 10:380S–384S